

Numerical Methods and Optimal Control for Glass Cooling Processes

G. Thömmes, R. Pinnau, M. Seaid, T. Götz, and A. Klar

Fachbereich Mathematik
Technische Universität Darmstadt
64289 Darmstadt
Germany
and
Fachbereich Mathematik
Universität Kaiserslautern
67663 Kaiserslautern
Germany

Abstract

In this paper, we discuss numerical and analytical approximations of radiative heat transfer equations used to model cooling processes of molten glass. Simplified diffusion type approximations are discussed and investigated numerically. These approximations are also used to develop acceleration methods for the iterative solution of the full radiative heat transfer problem. Moreover, applications of the above diffusion type approximations to optimal control problems for glass cooling processes are discussed.

1 Introduction

In glass manufacturing, a hot melt of glass is cooled down to room temperature. The annealing has to be monitored carefully in order to avoid excessive temperature differences which may affect the quality of the product or even lead to cracks in the material. In order to control this process it is, therefore, of interest to have a mathematical model that accurately predicts the temperature evolution. The model involves the direction-dependent thermal radiation field because significant part of the energy is transported by photons. Unfortunately, this fact makes the numerical solution of the radiative transfer equations much more complex, especially in higher dimensions, since, besides position and time variables, the directional variables also have to be accounted for, see [8, 4]. Therefore, a variety of different approximations of the full model that are computationally less time consuming but yet sufficiently accurate have been developed, see [1, 2, 3] and many others. Here, we discuss the SP_N approximations. These approximations may also be used to accelerate the solution of the full transfer equation. This is achieved using the SP_N approximations as preconditioner for the iterative solution method for the full equations. Finally, an important issue is the control of the annealing process as discussed above. We state and investigate the mathematical control problem.

The paper is organized in the following way. Section 2 contains a description of the radiative heat transfer equations used to model glass cooling processes. The associated SP_N approximations are stated in Section 3. Several numerical examples are shown comparing the approach to transport and diffusion models in one and multidimensional geometries. Section 4 describes an application of the P_1 model. It is used to accelerate the computation of the full transport problem by constructing a preconditioner for an iterative solver. Section 5 outlines the treatment of an optimal control problem in glass cooling processes with the above stated approximate equations as a second example for an application of the SP_N approximations.

2 The radiative heat transfer equations

To model glass cooling processes we consider the following coupled system of equations for temperature $T = T(x, t)$ and radiative intensity $I(x, t, \Omega, \nu)$, where $x \in \mathbb{R}^3$, $t \in [0, \infty)$, $\Omega \in S^2$, $\nu \in [0, \infty)$ are space, time, angle, and

frequency, respectively:

$$c_m \rho_m \partial_t T = \nabla \cdot (k_0 \nabla T) + \int_{\nu_1}^{\infty} \langle \sigma(I - B) \rangle d\nu$$

$$\forall \nu > \nu_1, \Omega \in S^2 : \quad \Omega \cdot \nabla I = \sigma(B - I).$$

$\sigma(\nu)$ denotes the absorption rate i.e. the opacity of the glass. We use the notation

$$\langle f \rangle = \int_{S^2} f(\Omega) d\Omega, \quad \text{for } f : S^2 \longrightarrow \mathbb{R}.$$

Planck's function B in glass is given by

$$B(T, \nu) = n_G^2 \frac{2h\nu^3}{c^2} \left(e^{\frac{h\nu}{kT}} - 1 \right)^{-1}$$

$$\int_0^{\infty} B(T, \nu) d\nu = n_G^2 a T^4, \quad a = \frac{2\pi^4 k_B^4}{15c^2 h^3} \quad (\text{Stefan-Boltzmann law}).$$

Boundary conditions are

$$k_0 n \cdot \nabla T = h_0(T_b - T) + \alpha \pi \left(\frac{n_L}{n_G} \right)^2 \int_0^{\nu_1} B(T_b, \nu) - B(T, \nu) d\nu$$

for the temperature and for inward pointing directions Ω (i.e. $n \cdot \Omega < 0$): we impose semi-transparent boundary conditions

$$I(\Omega) = \rho I(\Omega') + (1 - \rho) I_b(\Omega), \quad \text{with } \Omega' = \Omega - 2(n \cdot \Omega)n.$$

α, k_0, h_0 are constants, n_L, n_G are the refractive indices for air and glass. ρ denotes the reflective coefficient and T_b, I_b are outside temperature and outside radiative intensity, respectively.

Introducing the small parameter $\varepsilon = \frac{1}{\sigma_{ref} x_{ref}} \ll 1$ with reference absorption rate σ_{ref} and reference length x_{ref} , a scaling for optically thick material gives the following non-dimensional equations

$$\varepsilon^2 \partial_t T = \varepsilon^2 \nabla \cdot (k_0 \nabla T) + \int_{\nu_1}^{\infty} \langle \sigma(I - B) \rangle d\nu$$

$$\forall \nu > \nu_1, \Omega \in S^2 : \quad \varepsilon \Omega \cdot \nabla I = \sigma(B - I)$$

with boundary conditions

$$\varepsilon k_0 n \cdot \nabla T = h_0(T_b - T) + \alpha \pi \left(\frac{n_L}{n_G} \right)^2 \int_0^{\nu_1} B(T_b, \nu) - B(T, \nu) d\nu.$$

3 SP_N -Approximations

To approximate the equations given in the last section we proceed in the following way: Inverting

$$\left(1 + \frac{\varepsilon}{\sigma} \Omega \cdot \nabla\right) I = B$$

formally gives the asymptotic expansion for $\varepsilon \rightarrow 0$

$$4\pi B = \left[1 - \frac{\varepsilon^2}{3\sigma^2} \Delta - \frac{4\varepsilon^4}{45\sigma^4} \Delta^2 - \frac{44\varepsilon^6}{945\sigma^6} \Delta^3\right] \varphi + O(\varepsilon^8). \quad (1)$$

where we introduced $\varphi = \langle I \rangle$. Together with

$$\partial_t T = \nabla \cdot (k_0 \nabla T) + \frac{1}{\varepsilon^2} \int_{\nu_1}^{\infty} \sigma(\varphi - 4\pi B) d\nu$$

one obtains the SP_N -approximations, see [2, 7] for details: SP_1 is obtained including terms up to $O(\varepsilon^2)$ in (1), SP_2 for approximation up to $O(\varepsilon^4)$ and SP_3 for approximation up to $O(\varepsilon^6)$, respectively. The three approximate equations are stated in the following: The SP_1 -approximation is

$$\begin{aligned} \partial_t T &= \nabla \cdot (k_0 \nabla T) + \int_{\nu_1}^{\infty} \nabla \cdot \left(\frac{1}{3\sigma} \nabla \varphi\right) d\nu \\ \forall \nu > \nu_1 : \quad & -\varepsilon^2 \nabla \cdot \left(\frac{1}{3\sigma} \nabla \varphi\right) + \sigma \varphi = \sigma(4\pi B) \end{aligned} \quad (2)$$

with boundary conditions

$$\begin{aligned} \varepsilon k_0 n \cdot \nabla T &= h_0(T_b - T) + \alpha \pi \left(\frac{n_L}{n_G}\right)^2 \int_0^{\nu_1} B(T_b, \nu) - B(T, \nu) d\nu \\ \forall \nu > \nu_1 : \quad & \alpha_1 \varphi + \varepsilon \alpha_2 n \cdot \nabla \varphi = 4I_1. \end{aligned}$$

$\alpha_i, \beta_i, \mu_i, \gamma_i, \delta_i$ are constants depending on ρ , $I_i(x), \Gamma_i(x)$ depend on $I_b(x)$ at the boundary, see [2]. The SP_2 -approximation is

$$\begin{aligned} \partial_t T &= \nabla \cdot (k_0 \nabla T) + \int_{\nu_1}^{\infty} \nabla \cdot \left(\frac{1}{3\sigma} \nabla \xi\right) d\nu \\ \forall \nu > \nu_1 : \quad & -\varepsilon^2 \nabla \cdot \left(\frac{3}{5\sigma} \nabla \xi\right) + \sigma \varphi = \sigma(4\pi B) \end{aligned}$$

together with

$$\begin{aligned} \varepsilon k_0 n \cdot \nabla T &= h_0(T_b - T) + \alpha \pi \left(\frac{n_L}{n_G}\right)^2 \int_0^{\nu_1} B(T_b, \nu) - B(T, \nu) d\nu \\ \forall \nu > \nu_1 : \quad & \beta_1 \xi + \varepsilon \beta_2 n \cdot \nabla \xi = \beta_3 B + 4I_1 \end{aligned}$$

The SP_3 -approximation is

$$\begin{aligned}\partial_t T &= \nabla \cdot (k_0 \nabla T) + \int_{\nu_1}^{\infty} \nabla \cdot \frac{1}{\sigma} \nabla (a_1 \psi_1 + a_2 \psi_2) d\nu \\ \forall \nu > \nu_1 : & -\varepsilon^2 \mu_1^2 \nabla \cdot \left(\frac{1}{\sigma} \nabla \psi_1 \right) + \sigma \psi_1 = \sigma (4\pi B) \\ \forall \nu > \nu_1 : & -\varepsilon^2 \mu_2^2 \nabla \cdot \left(\frac{1}{\sigma} \nabla \psi_2 \right) + \sigma \psi_2 = \sigma (4\pi B)\end{aligned}$$

and

$$\begin{aligned}\varepsilon k_0 n \cdot \nabla T &= h_0 (T_b - T) + \alpha \pi \left(\frac{n_L}{n_G} \right)^2 \int_0^{\nu_1} B(T_b, \nu) - B(T, \nu) d\nu \\ \forall \nu > \nu_1 : & \gamma_1 \psi_1 + \gamma_2 \psi_2 + \varepsilon \gamma_3 n \cdot \nabla \psi_1 = \Gamma_1 \\ \forall \nu > \nu_1 : & \delta_1 \psi_1 + \delta_2 \psi_2 + \varepsilon \delta_3 n \cdot \nabla \psi_2 = \Gamma_2.\end{aligned}$$

Numerical results showing the temperature computed with the different models are presented in the following figures:

Figures 1 and 2 show the temperature for two different values of ε , i.e. $\varepsilon = 1$ and $\varepsilon = 0.01$, in a one-dimensional slab. We observe that the SP_N equations

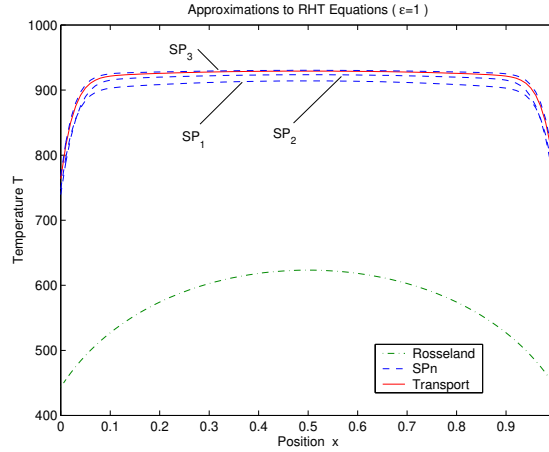


Figure 1: Comparison of the temperatures obtained by different approximations in the case of small absorption ($\varepsilon = 1$)

are good approximations to the full transport solution when compared with the solution of the classical diffusion or Rosseland equation. In particular, SP_3 is very accurate. Figure (3) shows a comparison of the approximation quality for different values of ε . Figures (4, 5) show the comparison for a 2-D computation of an infinite cylinder and a 3-D cube:

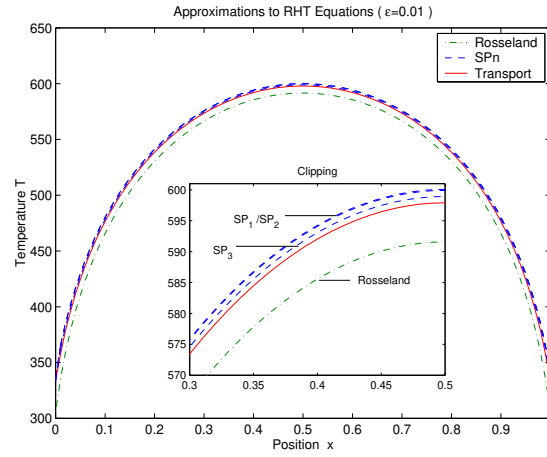


Figure 2: Comparison of the temperatures obtained by different approximations in the case of strong absorption ($\varepsilon = 0.01$)

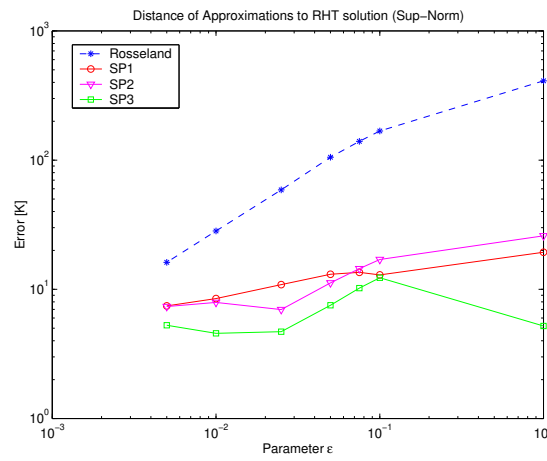


Figure 3: Approximation errors with respect to transport solution

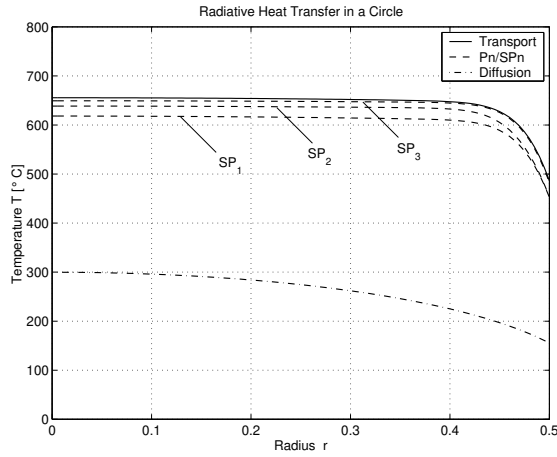


Figure 4: Comparison of the approximate models for a rotationally symmetric, infinite cylinder ($\varepsilon = 1$). The radial temperature distribution is shown.

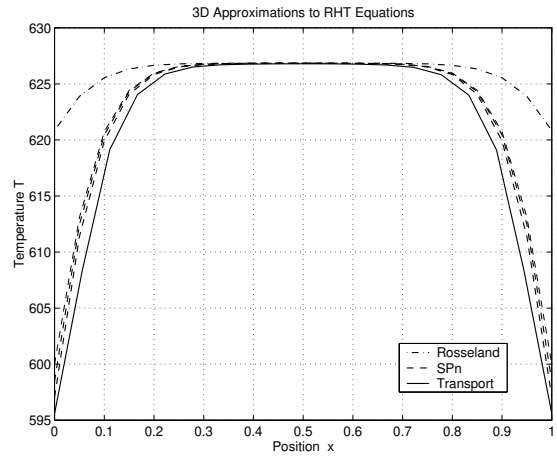


Figure 5: Comparison of the approximate models for a 3-D cube ($\varepsilon = 1$). The temperature along a line passing through the center of the cube is plotted.

4 Application I: Preconditioner for an Iterative Scheme for the RHT Equations

A semi-implicit scheme for the full time-dependent transport system is developed using the P_1 solution — analogous to the procedure used for the DSA method for neutron transport equations — as a preconditioner for the solution of the stationary equations which have to be solved in each time step. We refer to [6] for details. Consider, for simplicity, the frequency-independent transport equations for constant σ in 1-D slab geometry and use the new independent variable

$$B = n_G^2 a T^4, \quad B' = \frac{\partial B}{\partial T} = 4n_G^2 a T^3 \Big|_{T=T(B)}.$$

instead of T . This yields

$$\begin{aligned} \partial_t B &= (B') \partial_x \left(\frac{k_0}{(B')} \partial_x B \right) + \frac{1}{\varepsilon^2} (B') \sigma \langle I - B \rangle \\ \forall \mu \in [-1, 1] : \quad \varepsilon \mu \partial_x I &= \sigma (B - I) \end{aligned}$$

where we have in slab geometry

$$\langle f \rangle = \frac{1}{2} \int_{-1}^1 f(\mu) d\mu, \quad \text{for } f : [-1, 1] \longrightarrow \mathbb{R}.$$

A semilinear time discretization gives

$$\begin{aligned} \frac{B^{(n+1)} - B^{(n)}}{\Delta t} &= (B')^{(n)} \partial_x \left(\frac{k_0}{(B')^{(n)}} \partial_x B^{(n+1)} \right) + \frac{1}{\varepsilon^2} \sigma (B')^{(n)} \langle I^{(n+1)} - B^{(n+1)} \rangle \\ \varepsilon \mu \partial_x I^{(n+1)} &= \sigma (B^{(n+1)} - I^{(n+1)}) \end{aligned}$$

or formally in matrix notation

$$\begin{bmatrix} A_{11} & A_{12} \\ A_{21} & A_{22} \end{bmatrix} \begin{bmatrix} B^{(n+1)} \\ I^{(n+1)} \end{bmatrix} = \begin{bmatrix} B^{(n)} \\ 0 \end{bmatrix}.$$

A simple Block-Gauss-Seidel iteration leads to the solution of

$$\begin{aligned} B_0 &= B^{(n)}, \quad I_0 = I^{(n)}, \\ \begin{bmatrix} A_{11} & A_{12} \\ 0 & A_{22} \end{bmatrix} \begin{bmatrix} B_{k+1} \\ I_{k+1} \end{bmatrix} &= \begin{bmatrix} B^{(n)} \\ -A_{21} B_k \end{bmatrix} \end{aligned}$$

to determine $B^{(n+1)} = \lim_{k \rightarrow \infty} B_k$ and $I^{(n+1)} = \lim_{k \rightarrow \infty} I_k$. This is only a shorthand notation for the system

$$\begin{aligned} \left[\varepsilon^2 + \Delta t(B')^{(n)} 4\pi\sigma - \varepsilon^2 \Delta t(B')^{(n)} \partial_x \left(\frac{k_0}{(B')^{(n)}} \partial_x \right) \right] B_{k+1} \\ - \Delta t(B')^{(n)} \sigma \langle I_{k+1} \rangle = B^{(n)}, \end{aligned} \quad (3)$$

$$\left[\varepsilon\mu\partial_x + \sigma \right] I_{k+1} = \sigma B_k.$$

The errors

$$b_k = B^{(n+1)} - B_k, \quad i_k = I^{(n+1)} - I_k$$

fulfill

$$\begin{aligned} \left[\varepsilon^2 + \Delta t(B')^{(n)} 4\pi\sigma - \varepsilon^2 \Delta t(B')^{(n)} \partial_x \left(\frac{k}{(B')^{(n)}} \partial_x(\cdot) \right) \right] b_{k+1} \\ - \Delta t(B')^{(n)} \sigma \langle i_{k+1} \rangle = 0 \end{aligned} \quad (4)$$

$$\left[\varepsilon\mu\partial_x + \sigma \right] i_{k+1} = \sigma b_k.$$

We make an ansatz for the error in terms of Fourier modes:

$$b_k = \hat{b}_k e^{j\lambda x}, \quad i_k = \hat{i}_k e^{j\lambda x}.$$

where j denotes the imaginary unit ($j^2 = -1$). Inserting the Fourier modes in the above equation gives

$$\begin{aligned} \left[\varepsilon^2 + \Delta t(B')^{(n)} 4\pi\sigma - \varepsilon^2 k_0 \Delta t(j\lambda)^2 \right] \hat{b}_{k+1} - \Delta t(B')^{(n)} \sigma \langle \hat{i}_{k+1} \rangle = 0 \\ \left[\varepsilon\mu(j\lambda) + \sigma \right] \hat{i}_{k+1} = \sigma \hat{b}_k. \end{aligned}$$

Defining constants

$$C_1 = \Delta t(B')^{(n)} 4\pi\sigma, \quad C_2 = k_0 \Delta t, \quad \text{and} \quad \chi = \varepsilon^2 + C_1 + C_2 \varepsilon^2 \lambda^2,$$

the first equation may be shortly written

$$\hat{b}_{k+1} = \frac{C_1}{4\pi\chi} \langle \hat{i}_{k+1} \rangle.$$

Moreover, we can explicitly compute the total radiation

$$\langle \hat{i}_{k+1} \rangle = (\sigma \hat{b}_k) 2\pi \int_{-1}^{+1} \frac{d\mu}{\sigma + j\varepsilon\lambda\mu} = 4\pi \hat{b}_k \cdot \frac{1}{2} \int_{-1}^{+1} \frac{d\mu}{1 + j\frac{\varepsilon\lambda\mu}{\sigma}}.$$

The definite integral on the right has the value

$$S = \frac{1}{2} \int_{-1}^{+1} \frac{d\mu}{1 + j\frac{\varepsilon\lambda\mu}{\sigma}} = \frac{1}{2} \int_{-1}^{+1} \frac{d\mu}{1 + \left(\frac{\varepsilon\lambda\mu}{\sigma}\right)^2} = \frac{\sigma}{\varepsilon\lambda} \arctan \frac{\varepsilon\lambda}{\sigma},$$

such that we obtain

$$\langle \hat{i}_{k+1} \rangle = 4\pi\omega_0 \hat{b}_{k+1} = \frac{C_1}{\chi} \omega_0 \langle \hat{i}_k \rangle = \omega \langle \hat{i}_k \rangle.$$

where functions ω and ω_0 are defined by

$$\omega = \frac{C_1}{\chi} \omega_0, \quad \omega_0 = \frac{\sigma}{\sigma_s + \sigma} \frac{\arctan \Sigma}{\Sigma}, \quad \text{and} \quad \Sigma = \frac{\varepsilon\lambda}{\sigma}.$$

This may be summarized by the following 2×2 system for the evolution for the amplitude of a mode $e^{j\lambda x}$

$$\begin{bmatrix} \hat{b}_{k+1} \\ \langle \hat{i}_{k+1} \rangle \end{bmatrix} = \begin{bmatrix} \omega & 0 \\ \omega_0 & 0 \end{bmatrix} \begin{bmatrix} \hat{b}_k \\ \langle \hat{i}_k \rangle \end{bmatrix}$$

Crucial for the convergence is the spectral radius $\rho_0 \equiv |\omega|$ which fulfills:

$$\rho_0(\varepsilon, \lambda) < 1, \quad \text{but} \quad \lim_{\varepsilon \rightarrow 0} \rho_0(\varepsilon, \lambda) = 1 \quad \text{and} \quad \lim_{\lambda \rightarrow 0} \rho_0(\varepsilon, \lambda) = 1.$$

We conclude that the iteration converges. However, the smaller ε is the slower becomes this simple iteration. We suggest to use the SP_1 solution as a preconditioner. Let B_{k+1}, I_{k+1} be the solution of equation (3) as before. System (4) for the errors b_{k+1}, i_{k+1} is approximated using the associated SP_1 -approximation, which can be written in the form

$$\begin{aligned} \left[\varepsilon^2 - \varepsilon^2 \Delta t (B')^{(n)} \partial_x \left(\frac{k_0}{(B')^{(n)}} \partial_x \right) \right] \theta_{k+1} \\ - \frac{\varepsilon^2 \Delta t (B')^{(n)}}{3\sigma} \Delta \varphi_{k+1} = \Delta t (B')^{(n)} 4\pi\sigma (B_{k+1} - B_k), \\ -4\pi\sigma \theta_{k+1} + \left[-\frac{\varepsilon^2}{3\sigma} \partial_x^2 + \sigma \right] \varphi_{k+1} = 4\pi\sigma (B_{k+1} - B_k). \end{aligned}$$

and the corresponding solutions θ_{k+1} and ψ_{k+1} yield corrections for the iterates of the simple iteration. Given the old iterates B_k and I_k we update B_{k+1} and I_{k+1} by adding the correction terms in the following way

$$\begin{aligned} B_k &\longrightarrow B_{k+1} + \theta_{k+1} \\ \langle I_k \rangle &\longrightarrow \langle I_{k+1} \rangle + \psi_{k+1} \end{aligned}$$

An analogous analysis as before reveals in this case that the spectral radius is given by

$$\rho \equiv \rho(\varepsilon, \lambda) = \left| \omega(\varepsilon, \lambda) - \frac{1 - \omega(\varepsilon, \lambda)}{D(\varepsilon, \lambda)} \sigma C_1 \right|$$

where the function D is

$$D = \left(\sigma + \frac{\varepsilon^2}{3\sigma} \lambda^2 \right) \chi - \sigma C_1.$$

The spectral radius ρ has the properties

$$\rho(\varepsilon, \lambda) \leq \bar{\rho} < 1, \quad \lim_{\lambda \rightarrow 0} \rho(\varepsilon, \lambda) = 0, \quad \lim_{\varepsilon \rightarrow 0} \rho(\varepsilon, \lambda) = 0.$$

Consequently, the preconditioned iteration converges faster than the previous iteration. Moreover, it continues to converge sufficiently fast when ε approaches 0 while the simple iteration becomes increasingly slow, as mentioned above. Numerical experiments give the following results for the reduction of the errors of the Fourier modes (Fig. 6) and the convergence rates with respect to ε (Fig. 7): We observe that the convergence rates with preconditioning remain bounded away from 1 as ε tends to 0 in contrast to the case without preconditioning.

5 Application II: Optimal control of the temperature

The cooling of molten glass is performed slowly by controlling the outer temperature in a furnace. The specific way how the cooling down process is performed, in particular the local temperature gradients appearing during the process, strongly influences the quality of the glass.

One major objective in engineering applications is the reduction of local temperature gradients in the glass in order to reduce stresses and strains and

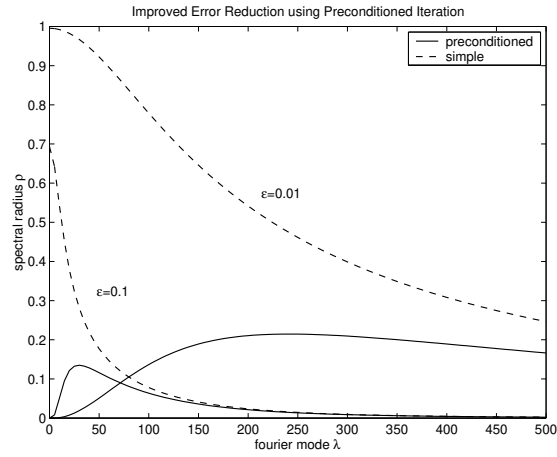


Figure 6: Comparison of the reduction of the amplitude of Fourier modes $e^{j\lambda x}$ of the error with and without preconditioning for $\varepsilon = 0.1$ and $\varepsilon = 0.01$

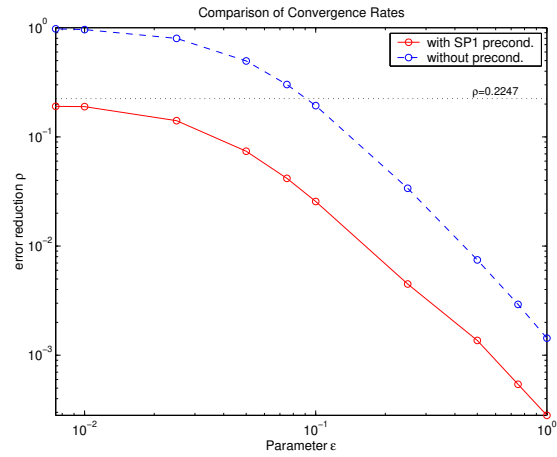


Figure 7: Convergence rates with and without preconditioning for various values of the parameter ε

possible breaking of glass. Moreover, a reduction of the cooling time reduces the energy necessary for the process.

To control this process along the desired state we consider cost functionals of tracking-type

$$J_1 = J_1(T, g, t_f) = \frac{1}{2} \int_0^{t_f} \|T - T_d\|_{L^2(\Omega)}^2 dt + \frac{\bar{\varepsilon}}{2} \int_0^{t_f} \|g - g_d\|_{L^2(\partial\Omega)}^2 dt + \frac{\bar{\delta}}{2} t_f^2$$

or

$$J_2 = J_2(T, g, t_f) = \frac{1}{2} \int_0^{t_f} \|\nabla T\|_{L^2(\Omega)}^2 dt + \frac{\bar{\varepsilon}}{2} \int_0^{t_f} \|g - g_d\|_{L^2(\partial\Omega)}^2 dt + \frac{\bar{\delta}}{2} t_f^2.$$

Here, t_f denotes the final time, T_d is a given desired temperature profile and g is the control parameter, i.e. the outside temperature. Further, g_d describes a given initial outer temperature profile at the boundary. The constants $\bar{\delta}$ and $\bar{\varepsilon}$ allow to adjust the weight of the cost and the observation. Clearly, J_2 will minimize the gradients in the temperature profile T , but also J_1 might yield this effect as T_d can be chosen constant in space.

The goal is to find minima of J under the condition that the temperature fulfills the radiative heat transfer system that models glass cooling. For the sake of simplicity, both from an analytical and a numerical point of view, we replace the RHT system by its SP_1 approximation. Hence, we minimize J under the following constraint, which represents the SP_1 model in a generic form

$$\partial_t T = \Delta T + \Delta \varphi \tag{6a}$$

$$-\Delta \varphi + \varphi = T^4 \tag{6b}$$

with boundary conditions

$$T + n \cdot \nabla T = g \tag{6c}$$

$$\varphi + n \cdot \nabla \varphi = g^4 \tag{6d}$$

Note, that all physical constants are set to one to simplify the notation.

In fact, we have to deal with a constrained optimization problem for the boundary control g .

To solve this problem numerically we derive the first-order optimality system via the Lagrange functional

$$\begin{aligned}
L(T, \varphi, g, t_f, \xi_T, \xi_\varphi) &= J(T, g, t_f) + \int_0^{t_f} \langle \partial_t T, \xi_T \rangle_{H^{-1}, H^1} dt \\
&+ \int_0^{t_f} \int_\Omega \nabla T \nabla \xi_T dx dt + \int_0^{t_f} \int_{\partial\Omega} (T - g) \xi_T ds dt \\
&+ \int_0^{t_f} \int_\Omega \nabla \varphi \nabla \xi_T dx dt + \int_0^{t_f} \int_{\partial\Omega} (\varphi - g^4) \xi_T ds dt \\
&+ \int_0^{t_f} \int_\Omega \nabla \varphi \nabla \xi_\varphi dx dt + \int_0^{t_f} \int_\Omega (\varphi - T^4) \xi_\varphi dx dt + \int_0^{t_f} \int_{\partial\Omega} (\varphi - g^4) \xi_\varphi ds dt.
\end{aligned}$$

where ξ_T and ξ_φ are Lagrange multiplier functions. For details see [5]. We consider here for simplicity only J_1 and assume that the final time t_f is fixed.

Clearly, the variation of L with respect to $\xi = (\xi_T, \xi_\varphi)$ yields the state system (6). Employing variations with respect to T and φ we derive the adjoint system for the Lagrange multipliers ξ_T, ξ_φ :

$$-\partial_t \xi_T = \Delta \xi_T - (4T^3) \xi_\varphi + (T - T_d) \quad (7a)$$

$$-\Delta \xi_\varphi + \xi_\varphi = \Delta \xi_T \quad (7b)$$

with homogeneous Robin boundary conditions for ξ_T and ξ_φ . This system is supplemented with the terminal condition

$$\xi_T(t_f, x) = \xi_\varphi(t_f, x) = 0. \quad (7c)$$

Finally, variations with respect to g yield the algebraic equation

$$\xi_T - \bar{\varepsilon}(g - g_d) + 4(\xi_T + \xi_\varphi)g^3 = 0 \quad \text{on } \partial\Omega \quad (8)$$

for $t \in (0, t_f)$.

We solve the first-order system (6),(7) and (8) iteratively, which can be interpreted as a variant of a gradient-descent algorithm. The optimality system for J_2 can be derived in analogy and variations with respect to t_f are straight forward yielding another algebraic relation for the final time t_f .

Numerical results for the cost functional J_1 with optimization of final time t_f , i.e. $\bar{\delta} \neq 0$, are plotted in Fig 8. For reference the given boundary temperature profile g_d is also plotted there. The desired state T_d is constant in space having the boundary values g_d . Note that one gains 20 % of time while the local temperature gradients are almost unchanged.

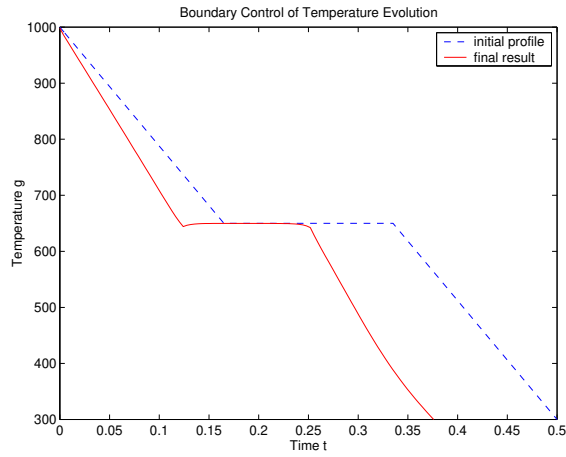


Figure 8: Minimization of $\|T - T_d\|_2$ (with optimization of final time)

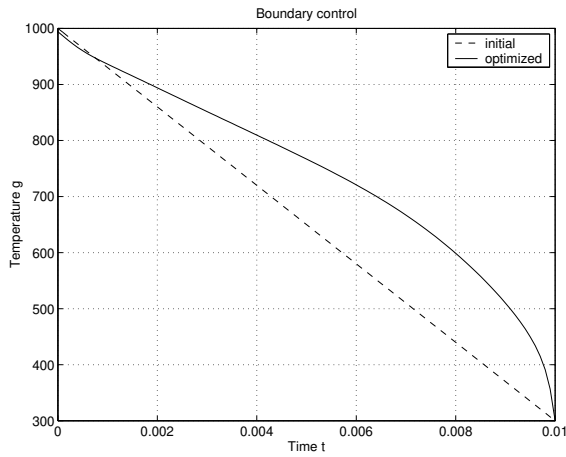


Figure 9: Minimization of $\|\nabla T\|_2$ (without optimization of final time)

The results for the cost functional J_2 with fixed final time ($\bar{\delta} = 0$) are given in Fig 9. In table 1 we present the values of the cost and the observation for several values of $\bar{\varepsilon}$. Clearly, the mean value norm of the gradient is decreasing by increasing costs. Note, that also the maximum norm of the gradient is decreasing, which underlines the reasonability of the choice of J_2 .

ε	J	$\ g - g_d\ _2$	$\ \nabla T\ _2$	$\ \nabla T\ _\infty$
-	22.6901	0	6.7365	344.8252
1	22.0623	0.6044	6.6151	343.8816
0.5	21.4694	1.1849	6.4990	343.5875
0.1	17.7177	5.1592	5.7248	342.0602
0.05	14.4975	8.9485	4.9991	341.4265

Table 1: Minimization of $\|\nabla T\|_2$. Value of the functional and norms of boundary control and gradient of the temperature for varying ε .

6 Conclusions:

- The SP_N equations are simple yet accurate approximations of the full transport solutions.
- They can be used, for example, in order to accelerate the solution of the full radiative heat transfer equations or for control of glass cooling processes.

Acknowledgements:

This research was supported by the German research foundation (DFG Kl 1105/7 and SFB 568).

References

- [1] E. Larsen, G. Pomraning, and V.C. Badham. Asymptotic analysis of radiative transfer problems. *J. Quant. Spectr. and Radiative Transfer*, 29:285–310, 1983.

- [2] E. W. Larsen, G. Thömmes, and A. Klar. Simplified P_N Approximations to the Equations of Radiative Heat Transfer in Glass I: Modelling. *submitted*, 2001.
- [3] F.T. Lentes and N. Siedow. Three-dimensional radiative heat transfer in glass cooling processes. *Glastech. Ber. Glass Sci. Technol.*, 72:188–196, 1999.
- [4] M.F. Modest. *Radiative Heat Transfer*. McGraw-Hill, 1993.
- [5] R. Pinnau and G. Thömmes. Optimal boundary control of glass cooling processes. *submitted*, 2001.
- [6] G. Thömmes. An iterative scheme for the fast solution of the rht equations for glass in 1d. *submitted*, 2001.
- [7] G. Thömmes, T. Götz, M. Seaïd, A. Klar, and E. W. Larsen. Simplified P_N Approximations to the Equations of Radiative Heat Transfer in Glass II: Numerics. *submitted*, 2001.
- [8] R. Viskanta and E.E. Anderson. Heat transfer in semitransparent solids. *Advances in Heat Transfer*, 11:318, 1975.